Inversion of Pn travel times for lateral variations of moho geometry beneath the central Andes and comparison with the receiver functions

David Baumont, Anne Paul, George Zandt, Susan L. Beck

GEOPHYSICAL RESEARCH LETTERS, VOL. 28, NO. 8, PAGES 1663-1666, APRIL 15, 2001

Inversion of *Pn* travel times for lateral variations of Moho geometry beneath the Central Andes and comparison with the receiver functions

David Baumont and Anne Paul
Laboratoire de Géophysique Interne et Tectonophysique, Centre National de la Recherche Scientifique and Université Joseph Fourier, Grenoble, France.

George Zandt and Susan L. Beck
Southern Arizona Seismological Observatory and Department of Geosciences, University of Arizona, Tucson, Arizona, USA.

Abstract. We inverted the *Pn* travel times to characterize the geometry of the Moho along a profile across the Central Andes (20°S) where previous workers have estimated the crustal thickness using receiver functions. Contrary to receiver functions, this technique is not sensitive to the crustal V_s. Therefore, the comparison of the two approaches provides valuable complementary information. Overall, our results are in good agreement with those based on receiver functions. However, some important discrepancies are observed beneath the Western Cordillera and the Subandes, where we find crusts 10-km thinner than in previous models. We confirm that the central part of the orogen appears to be isostatically compensated by the presence of a thick crust. However, at both edges, the topography probably requires additional support, low-density mantle beneath the Western Cordillera and a strong flexural support of the Brazilian shield beneath the Subandes.

Introduction

The receiver function technique has been extensively used in the last decades to estimate the crustal thickness especially in remote areas as it is both efficient and rather straightforward for a moderate cost. However, this technique requires to estimate the V_p/V_s ratio (for example from multiple reflections) which is not always possible. We present here a complementary technique to image the lateral variations of the Moho geometry based on a *Pn* travel time inversion, a technique that does not depend on V_s, and compare the results with those based on a receiver function analysis to evaluate the tradeoffs in V_s and depth.

From June to November 1994, two complementary seismological networks were deployed across the main morphotectonic units of the Central Andes along the same profile (Figure 1a). The 1/2 year Lithoscope experiment [*Dorbath et al.*, 1996] involved 56 short-period stations that were interpersed with the 16 broadband stations of the 1 and 1/2 year BANJO (Broadband ANdean JOint) experiment [*Beck et al.*, 1996] resulting in a dense east-west profile across the entire range. From these data, *Beck et al.* [1996] estimated the Moho geometry using a receiver function analysis, reporting strong

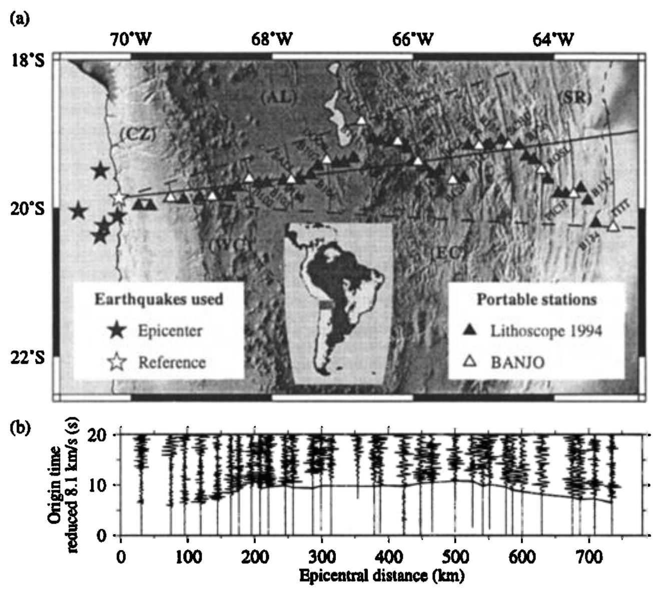

Figure 1. (a) Topographic map of the Central Andes showing the locations of the stations (triangles) and earthquakes (stars) used in this study. Station names are written only for stations used in this study. The aperture of the profile along its mean axis (solid line) through the reference earthquake epicenter (white star) is delineated by the long-dashed line. The arcs of circles represent the *Pn* wavefront. The main morpho-tectonic units are from west to east: Coastal Zone (CZ), Western Cordillera (WC), Altiplano (AL), Eastern Cordillera (EC), Subandean Range (SR). (b) Vertical component record section of the reference crustal earthquake (white star in Figure 1a). A reduction velocity of 8.1 km/s has been used. The *Pn* travel time curve is shown by the solid line.

Paper number 2000GL011720.
0094-8276/01/2000GL011720$05.00

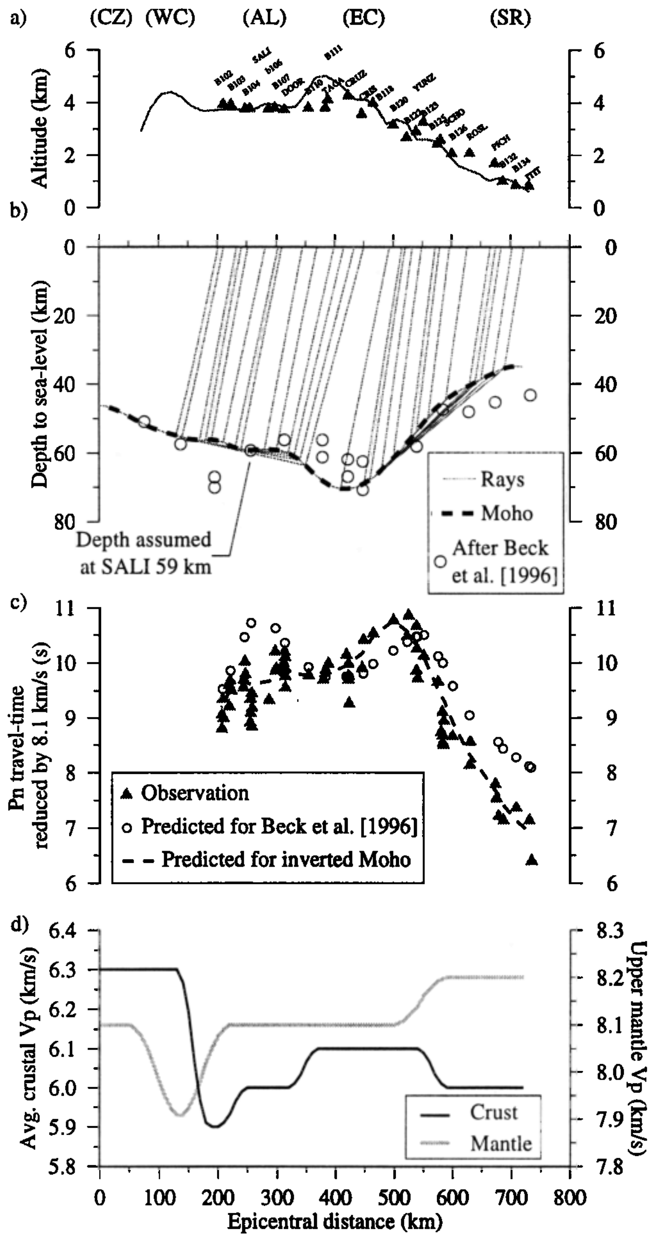

Figure 2. (a) Topography of the Central Andes along the profile. (b) Geometry of the Moho resulting from the inversion of *Pn* travel times (dashed line) and inferred by *Beck et al.* [1996] (circles) after conversion using our assumption of the lateral variations of the average crustal V_p (shown in Figure 2d). *Pn* raypaths (thin lines) are only shown to illustrate the relationship between a station and the emission point of the *Pn* at the Moho. (c) Fit between observed (triangles) and predicted *Pn* travel times for the inverted geometry of the Moho (dashed line) and the Moho inferred by *Beck et al.* [1996] (circles). (c) Lateral variations of the average velocity models modified from Wigger et al. [1994] and used in the Moho inversion.

lateral changes in crustal thickness. However, recent studies have documented strong lateral variations of the V_p/V_s ratio [*Dorbath and Masson*, 2000] and crustal V_s [*Baumont et al.*, 2001] along the same profile, strengthening the need for an estimate of the crustal thickness using a technique independent of the V_p/V_s ratio. This opportunity is provided by the recording of *Pn* arrivals by the densely spaced (15 km) networks mentionned above.

Determination of *Pn* travel times

During the overlapping period of the deployments, several crustal earthquakes were recorded and located by *Masson et al.* [2000] with a 3 km standard error. We selected events more or less aligned with the profile (Figure 1a) to simplify the problem to a 2D propagation geometry.

For each earthquake, after removing the instrument response, we picked the *Pn* arrival on band-pass filtered or raw signals depending on their quality and we estimated an uncertainty on each observation. To better identify the *Pn* from the *Pg*, we conducted numerical computations of their travel times for a realistic Moho geometry of the Andes based upon the receiver function analysis by *Beck et al.* [1996]. As we found that *Pn* arrives first beyond 180 km in this model, and the slope of the observed hodochron of the first arrivals changes at about 200 km, we only considered picks for epicentral distances larger than 200 km. A vertical component record section for one of the selected earthquakes is shown in Figure 1b and displays strong lateral variations of the *Pn* apparent velocity.

To prevent any bias due to bad depth locations or bad origin time determination, we restrained our analysis to the differential time of *Pn*. Moreover, to increase the robustness of the dataset, we combined all differential *Pn* travel times observed for all events. Dataset were assembled preserving the measurements of *Pn* apparent velocity and their locations along the median profile. This was achieved by choosing a reference event (see location in Figure 1a) and adjusting in the least square sense the observed travel times in both time and space.

The dataset includes 65 picks from 5 events at 25 stations. As shown in Figure 2c, reduced *Pn* travel times observed along the network spread over 4 s suggesting the existence of large lateral variations of the Moho geometry and/or the crustal and upper mantle V_p.

Inversion of *Pn* travel times for Moho geometry

Pn travel times recorded for natural sources are of common use to image the upper mantle V_p [e.g. *Hearn et al.*, 1991], or both upper mantle V_p and Moho geometry [e.g. *Shearer and Oppenheimer*, 1982; *Hearn and Clayton*, 1986; *Hearn and Rosca*, 1994]. In these studies, Moho variations are assumed to be a second order parameter relative to velocity. However, the Central Andes are characterized by large variations of the crustal thickness [*Beck et al.*, 1996; *Wigger et al.*, 1994], and tests showed that the sensitivity of the *Pn* travel times to V_p models is weak in comparison to changes in Moho depth. Moreover, due to the lack of reverse profile, we could not invert for both velocity and Moho depth variations. We therefore inverted *Pn* travel times for the Moho geometry in a velocity model based on refraction studies by *Wigger et al.* [1994] (see Figure 2d).

We solved the direct problem of the *Pn* travel time calculation [*Baumont,* 1999] by ray tracing for given crustal and upper mantle V_p, Moho geometry, origin time and location of the source, and station elevations. No vertical variations of P wave velocity were taken in consideration in the crust and upper mantle. Using a flat Moho starting model, we computed differences between observed and predicted travel times. To minimize these misfits in the least-square sense, we wrote a simplified Jacobian matrix of the inverse problem where the unknowns are the Moho geometry and the reference origin time. Misfits were directly converted into variations of Moho depth by neglecting the lateral shifts of *Pn* emission points on the Moho. As *Pn* is very sensitive to the local slope of the Moho, we inverted for a smooth Moho geometry. Further tests with more complicated starting Moho geometries showed that our solution is not dependent on the starting model.

As we only consider the differential travel time to be significant, the absolute depth of the Moho cannot be determined. Consequently, we added a constraint on its depth at station SALI (Figure 1a) based upon the results of *Beck et al.* [1996] using a receiver function analysis at this same station. This observation was chosen because it shows no azimuthal dependence in the receiver functions. Moreover, this station is located in the Altiplano where tradeoffs between Moho depths and crustal average velocity are limited due to good knowledge of the average crustal V_p-to-V_s ratio [*Beck et al.,* 1996; *Swenson et al.,* 2000] and average crustal V_p [*Zandt et al.,* 1996; *Dorbath and Masson,* 2000].

To reduce the influence of bad *Pn* picks, we applied a constant low weight to the data with a difference between predicted and observed travel time larger than 1.8 times the standard deviation of the observations. About 5% of the data are concerned by this weighting which has a weak effect on the results.

Results

The Moho depth profile resulting from this inversion is presented in Figure 2b (thick dashed line) where it is also compared to *Beck et al.'s* [1996] results (open circles). Regarding the *Pn* arrival times, the misfit between observations and predictions is significantly smaller for our model (0.11 s^2) than for *Beck et al.'s* [1996] Moho geometry (0.74 s^2). Figure 2c documents this overall good fit between predicted (dashed line) and observed (triangles) travel times, except at station SALI where a 0.5 s difference is not modeled. The large difference in travel times between SALI and its neighbor B104 suggests a strong, short wavelength variation in Moho geometry beneath the eastern flank of the Western Cordillera, which is not modeled due to the smoothing criteria applied on the Moho geometry.

Beneath the eastern flank of the Western Cordillera and most of the Altiplano, the Moho is rather flat. Note the slight indication of crustal thinning under the Western Cordillera constrained by *Pn* arrival times at stations B102, B103, and B104. The crust thickens beneath the eastern part of the Altiplano and the highest peaks of the Eastern Cordillera with a Moho depth varying from 59 to about 70 km. From CRUZ [Figure 1a] located at the highest elevation of the Eastern Cordillera towards its eastern limit, the crust thins abruptly as the elevation goes down and the Moho depth changes from 70 to about 40 km. Beneath the Subandean range, the Moho depth is between 40 and 32 km. Except in the Western Cordillera, the Moho geometry is anticorrelated with the topography. We checked that all these results are only weakly affected by the assumptions on the velocity models.

Discussion

As *Pn* travel times are not sensitive to crustal V_s, this inversion is a powerful tool to evaluate the tradeoffs between crustal thickness and crustal velocities in the receiver function analysis. Our approach is mostly sensitive to the Moho geometry, the crustal V_p, and to a lesser extent to the upper mantle V_p. By contrast, the receiver function analysis is sensitive to the Moho depth and both the crustal average V_p and V_s. Differences in Moho geometries estimated using these two techniques may therefore reflect our lack of knowledge of the crustal V_s.

As shown in Figure 2b, our Moho geometry is overall in good agreement with the results of *Beck et al.* [1996]. However, some important discrepancies are observed locally. Beneath the eastern flank of the Western Cordillera, and beneath the eastern part of the Eastern Cordillera and the Subandean range, *Beck et al.* [1996] inferred a crustal thickness about 10 km larger than in our results. As shown in Figure 2c, these differences are related to significant misfits between *Pn* travel times observed and predicted from the model of *Beck et al.* [1996]. Beneath the Cordilleras, the discrepancies are probably due to anomalous V_p/V_s ratios as low V_s anomalies were reported by *Baumont et al.* [2001] by inverting the dispersion curves of surface waves. If so, the Moho depth deduced from the Ps-to-P delay in the receiver functions would have been overestimated, resulting in a decrease of the differences between the two approaches. Beneath the Subandean range, the V_p/V_s ratio is not very well known, however in this area, *Baumont et al.* [2001] did not report any low crustal V_s anomalies. In this case, the discrepancies may result from both crustal V_p and V_s anomalies. In addition, the divergence of the subandean stations from the radial axis of the network might violate the 2-D structure assumption, and contribute to part of the observed discrepancy. Using a combination of both receiver function analysis and *Pn* travel time inversion is a powerful approach and would yield more reliable results by reducing the tradeoffs.

A relatively thin crust beneath the Western Cordillera would likely rule out an entirely isostatic compensation due to the presence of a thick crustal root. The topography could then rather be supported by a localized low-density mantle related to the volcanic activity. Such a feature is qualitatively consistent with the lithospheric V_s cross-section proposed by *Baumont et al.* [2001] where a thin lithospheric lid was found under the Western Cordillera. In the Subandes where we find a thinner crust than previous workers [*Beck et al.*, 1996; *Wigger et al.*, 1994], the topography is probably partly supported by the flexural rigidity of the underlying Brazilian shield as proposed by *Lyon-Caen et al.* [1985] based on gravity.

Acknowledgments. The Lithoscope projects were funded by ORSTOM and INSU-CNRS. Funding for the BANJO experiment was provided by NSF grants EAR-9304949, EAR-9614250 and EAR-9304560 at the University of Arizona and Carnegie Institution of Washington, respectively. This work has been partly supported by ATP Tomographie 1996 of INSU/CNRS. We would like to thank all the members of the field crews. Calculations were performed at the Centre de Calcul Intensif de l'Observatoire de Grenoble. We are grateful to the Editor, Dr Kiyoshi Suyehiro, for sorting out the administrative problems during processing of this manuscript.

References

Baumont, D., Caractérisation sismologique de la structure lithosphérique des Andes centrales (17° - 20°S), PhD thesis, Université Joseph Fourier, Grenoble, France, 1999.

Baumont, D., A. Paul, G. Zandt, S. L. Beck, and H. Pedersen, Lithospheric Structure of the Central Andes Based on Surface Wave Dispersion, Submitted to *J. Geophys. Res.*

Beck, S. L., G. Zandt, S. C. Myers, T. C. Wallace, P. G. Silver, and L. Drake, Crustal-thickness variations in the Central Andes, *Geology, 24,* 407-410, 1996.

Dorbath, C., A. Paul, and The Lithoscope Andean Group, Tomography of the Andean crust and mantle at 20°*S*: first results of the Lithoscope experiment, *Phys. Earth Planet. Int., 97,* 133-144, 1996.

Dorbath, C., and F. Masson, Composition of the crust and upper-mantle in the Central Andes (19°30'S) inferred from P wave velocity and Poisson's ratio, *Tectonophysics, 327,* 213-223, 2000.

Hearn, T., and R. Clayton, Lateral velocity variations in southern California. II. Results for the lower crust from *Pn* waves, *Bull. Seism. Soc. Am., 76,* 511-520, 1986.

Hearn, T., N. Beghoul, and M. Barazangi, Tomography of the Western United States from the regional arrival times, *J. Geophys. Res., 96,* 16,369-16,381, 1991.

Hearn, T., and A. Rosca, *Pn* tomography beneath the Southern Great Basin, *Geophys. Res. Lett., 21,* 2187-2190, 1994.

Lyon-Caen, H., P. Molnar, and G. Suárez, Gravity anomalies and flexure of the Brasilian Shield beneath the Bolivian Andes, *Earth Planet. Sci. Lett, 75,* 81-92, 1985.

Masson F., C. Dorbath, C. Martinez and, G. Carlier, Local earthquake tomography of the Andes at 20°S - Implication for the structure and building of the chain, *J. of South America Earth Sciences, 13,* 3-19, 2000.

Shearer P., and D. Oppenheimer, A dipping Moho and crustal low-velocity zone from *Pn* arrivals at the Geysers-Clear Lake, California, *Bull. Seism. Soc. Am., 72,* 1551-1566, 1982.

Swenson J., S. L. Beck, and G. Zandt, Crustal structure of the Altiplano from broadband regional waveform modeling: Implications for the composition of thick continental crust, *J. Geophys. Res., 105,* 607-621, 2000.

Wigger, P., M. Schmitz, M. Areneda, G. Asch, S. Baldzuhn, P. Giese, W-D. Heinsohn, E. Martinez, E. Ricaldi, P. Rower, and P. Viramonte, Variation in the crustal structure of the southern Central Andes deduced from seismic refraction investigations, in *Tectonics of the southern Central Andes*, edited by K-J. Reutter, E. Scheuber and P. J. Wiggers, Springer, New York, 23-48, 1994.

Zandt G., S. L. Beck, S. R. Ruppert, C. J. Ammon, D. Rock, E. Minaya, T. C. Wallace, and P. G. Silver, Anomalous crust of the Bolivian Altiplano, Central Andes: Constraints from broadband regional seismic waveforms, *Geophys. Res. Lett., 23,* 1159-1162, 1996.

D. Baumont, and A. Paul, Laboratoire de Géophysique Interne et Tectonophysique, BP 53, F-38041 Grenoble, Cedex 9, France. (e-mail: dbaumont@obs.ujf-grenoble.fr; apaul@obs.ujf-grenoble.fr)

S. Beck, and G. Zandt, Southern Arizona Seismological Observatory and Department of Geosciences, University of Arizona, Tucson, AZ 85721. (e-mail: beck@geo.arizona.edu; zandt@geo.arizona.edu)

(Received April 25, 2000; revised January 12, 2001; accepted January 29, 2001.)